What about the shear normal stresses, Ψ_1 ,Ψ_2 from capillary data?

Extrudate swell - relation to N_1 is model dependent (see discussion in Macosko, p254)

$$N_1^2 = 8\tau_R^2\left(\left(\frac{D_e}{2R}\right)^6 - 1\right)$$

Assuming unconstrained recovery after steady shear, K-BKZ model with one relaxation time

$D_e =$ Extrudate diameter

Not a great method; can perhaps be used to index materials

Ψ_2 ? (cannot obtain from capillary flow, but…)

Macosko, Rheology: *Principles, Measurements, and Applications*, VCH 1994.

38

© Faith A. Morrison, Michigan Tech U.

We can obtain Ψ_1 ,Ψ_2 from slit-flow data: **Hole Pressure-Error**

Pressure transducers mounted in an access channel (hole) do not measure the same pressure as those that are “flush-mounted”:

$$\delta p_h \equiv p_{flush} - p_{hole}$$

Slot transverse to flow: $N_1 = 2\delta p_h\left(\frac{d\ln\delta p_h}{d\ln\tau_w}\right)$

Slot parallel to flow: $N_2 = -\delta p_h\left(\frac{d\ln\delta p_h}{d\ln\tau_w}\right)$

Circular hole: $N_1 - N_2 = 3\delta p_h\left(\frac{d\ln\delta p_h}{d\ln\tau_w}\right)$

Hou, Tong, deVargas, Rheol. Acta 1977, 16, 544

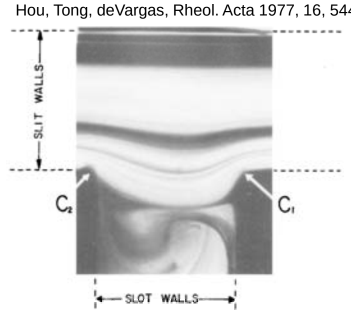

Fig. 4. Photograph of streamlines showing curvature near the mouth of a hole of slit cross-section for polyethylene (NPE 952) melts. Direction of flow is from right to left. Flow rate ≃ 0.02 ml/sec; shear rate at the wall ≃ 3.2 sec^{-1}; $d = 0.05$ in

(We can of course obtain η also from slit-flow data; the equations are analogous to the capillary flow equations)

Lodge, in *Rheological Measurement,* Collyer, Clegg, eds. Elsevier, 1988
Macosko, Rheology: *Principles, Measurements, and Applications*, VCH 1994.

39

© Faith A. Morrison, Michigan Tech U.

Limits on Measurements: Flow instabilities in rheology

capillary flow

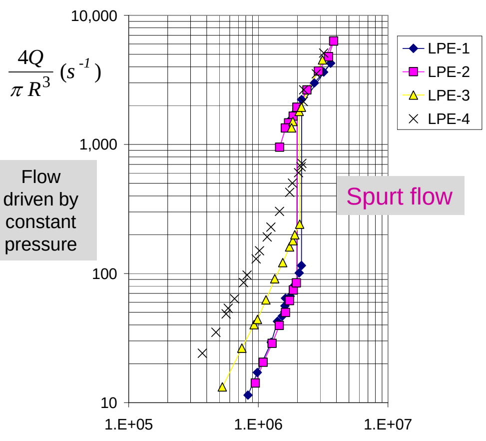

$\frac{4Q}{\pi R^3}\ (s^{-1})$

$\frac{\Delta P R}{2L},\quad dynes/cm^2$

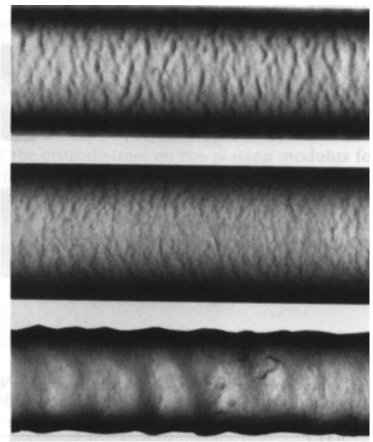

Figure 6.9, p. 176 Pomar et al. LLDPE

40

Figure 6.10, p. 177 Blyler and Hart; PE

© Faith A. Morrison, Michigan Tech U.

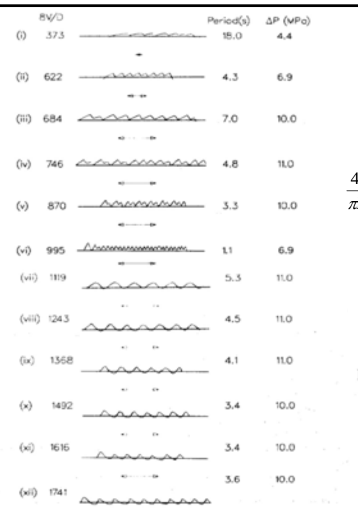

Fig. 11. Force vs. time curves; L/D = 100.1. Slip-stick region. The time interval indicated by the arrow below each curve equals ten seconds. Polymer was added to the reservoir after run (vi).

Limits on Measurements: Flow instabilities in rheology

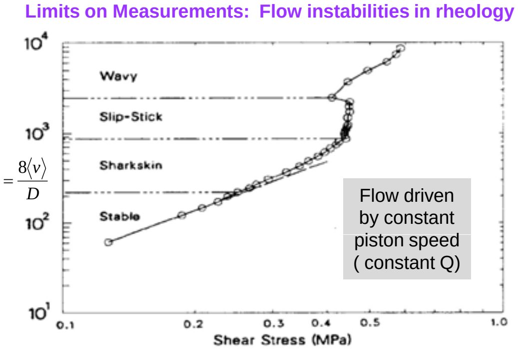

$\frac{4Q}{\pi R^3} = \frac{8\langle v\rangle}{D}$

Fig. 2. Uncorrected capillary data for LLDPE at 215°C, L/D = 33.2.

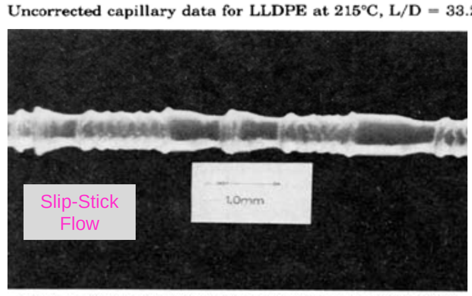

Fig. 8. LLDPE extrudate: transition region observed in slip-stick flow region. 8 V/D = 985; L/D = 100.1.

D. Kalika and M. Denn, *J. Rheol*. 31, 815 (1987)

© Faith A. Morrison, Michigan Tech U.

Torsional Parallel Plates

Viscometric flow

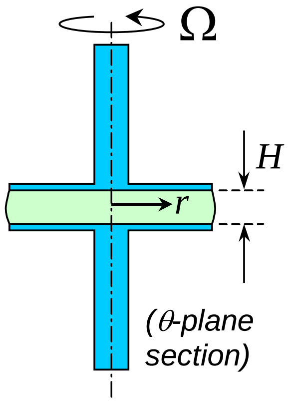

$$\underline{v} = \begin{pmatrix} 0 \\ v_\theta(r,z) \\ 0 \end{pmatrix}_{r\theta z}$$

42

© Faith A. Morrison, Michigan Tech U.

To calculate shear rate:

$$\underline{v} = \begin{pmatrix} 0 \\ A(r)z + B(r) \\ 0 \end{pmatrix}_{r\theta z}$$

$$v_\theta = A(r)z + B(r)$$

$$v_\theta = \frac{r\Omega z}{H}$$ (due to boundary conditions)

$$\dot{\gamma} = \left|\dot{\underline{\underline{\gamma}}}\right| = \left| \begin{pmatrix} 0 & \frac{\partial v_\theta}{\partial r} - \frac{v_\theta}{r} & 0 \\ \frac{\partial v_\theta}{\partial r} - \frac{v_\theta}{r} & 0 & \frac{\partial v_\theta}{\partial z} \\ 0 & \frac{\partial v_\theta}{\partial z} & 0 \end{pmatrix}_{r\theta z} \right|$$

$$\dot{\gamma} = ?$$

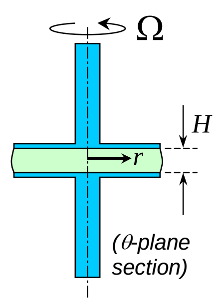

43

© Faith A. Morrison, Michigan Tech U.

Result: $\underline{v} = \begin{pmatrix} 0 \\ \frac{r\Omega z}{H} \\ 0 \end{pmatrix}_{r\theta z}$ $\quad \dot{\gamma} = \frac{r\Omega}{H}$

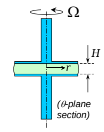

To calculate shear stress, look at EOM:

$$P \equiv p - \rho g z$$

$$\rho\left(\cancel{\frac{\partial \underline{v}}{\partial t}} + \cancel{\underline{v}\cdot\nabla\underline{v}}\right) = -\nabla P - \nabla\cdot\underline{\underline{\tau}}$$

steady state

neglect inertia

$$\underline{\underline{\tau}} = \begin{pmatrix} \tau_{rr} & 0 & 0 \\ 0 & \tau_{\theta\theta} & \tau_{\theta z} \\ 0 & \tau_{z\theta} & \tau_{zz} \end{pmatrix}_{r\theta z}$$

(viscometric flow)

$$\begin{pmatrix} 0 \\ 0 \\ 0 \end{pmatrix}_{r\theta z} = \begin{pmatrix} -\frac{\partial P}{\partial r} \\ 0 \\ -\frac{\partial P}{\partial z} \end{pmatrix}_{r\theta z} - \begin{pmatrix} \frac{1}{r}\frac{\partial r\tau_{rr}}{\partial r} - \frac{\tau_{\theta\theta}}{r} \\ \frac{\partial \tau_{z\theta}}{\partial z} \\ \frac{\partial \tau_{zz}}{\partial z} \end{pmatrix}_{r\theta z}$$

Assume:
- Form of velocity
- no θ-dependence
- symmetric stress tensor
- neglect inertia
- no slip
- isothermal

© Faith A. Morrison, Michigan Tech U.

Result: $$\frac{\partial \tau_{z\theta}}{\partial z} = 0$$

$$\tau_{z\theta} = f(r)$$

The experimentally measurable variable is the torque to turn the plate:

$$\underline{T} = \iint_S \left[\underline{R} \times \left(\hat{n}\cdot -\underline{\underline{\Pi}}\right)\right]_{surface} dS$$

$$\underline{T} = \int_0^{2\pi}\int_0^{R} \left[r\hat{e}_r \times \left(\hat{e}_z \cdot -\underline{\underline{\Pi}}\right)\right]_{z=H} r\,dr\,d\theta$$

$$T_z = 2\pi \int_0^R \left[-\tau_{z\theta}\right]_{z=H} r^2 dr$$

Following Rabinowitsch, replace stress with viscosity, r with shear rate, and differentiate.

© Faith A. Morrison, Michigan Tech U.

Torsional Parallel-Plate Flow - Viscosity

Measureables:
Torque **T** to turn plate
Rate of angular rotation **Ω**

Note: shear rate experienced by fluid elements depends on their r position. (consider effect on complex fluids)

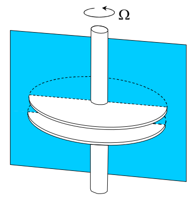

cross-sectional view:

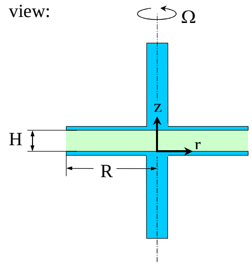

$$\dot{\gamma} = \frac{r\Omega}{H} = \dot{\gamma}_R \frac{r}{R}$$

By carrying out a Rabinowitsch-like calculation, we can obtain the stress at the rim (r=R).

$$\tau_{z\theta}\big|_{r=R} = -T/2\pi R^3 \left[3 + \frac{d\ln(T/2\pi R^3)}{d\ln\dot{\gamma}_R}\right]$$

$$\boxed{\eta(\dot{\gamma}_R) = \frac{-\tau_{z\theta}\big|_{r=R}}{\dot{\gamma}_R}}$$

Correction required

46

© Faith A. Morrison, Michigan Tech U.

Torsional Parallel-Plate Flow - correction

$$\frac{T}{2\pi R^3}$$

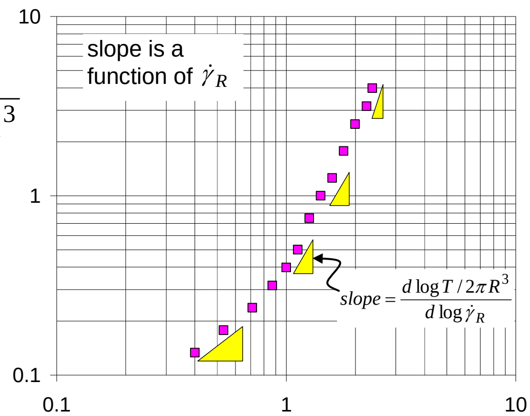

$$\dot{\gamma}_R = \frac{R\Omega}{H}$$

$$\boxed{\eta(\dot{\gamma}_R) = \frac{T/2\pi R^3}{\dot{\gamma}_R}\left[3 + \frac{d\ln(T/2\pi R^3)}{d\ln\dot{\gamma}_R}\right]}$$

47

© Faith A. Morrison, Michigan Tech U.

Torsional Parallel-Plate Flow – Viscosity – Approximate method

$$\tau_{z\theta}\Big|_{r=R} = -T/2\pi R^3 \left[3 + \frac{d\ln(T/2\pi R^3)}{d\ln\dot{\gamma}_R} \right]$$

=1 for Newtonian

$$-\tau_a \equiv \frac{2T}{\pi R^3}$$

For many materials: $\frac{d\ln(T/2\pi R^3)}{d\ln\dot{\gamma}_R} < 1.4$

$$\eta(\tau) = \eta_a(\tau_a) \pm 2\%$$

$$\tau = \tau_a(r = 0.76R)$$

Giesekus and Langer Rheol. Acta, 16, 1 1977

$$\boxed{\eta(\dot{\gamma}_{0.96R}) = \frac{-\tau_{0.76R}}{\dot{\gamma}_{0.76R}}}$$

No correction required

(but making a material assumption)

Macosko, Rheology: *Principles, Measurements, and Applications*, VCH 1994, p220

48

© Faith A. Morrison, Michigan Tech U.

Torsional Parallel-Plate Flow – Normal Stresses

Similar tactics, logic (see Macosko, p221)

$$\boxed{\left(N_1 - N_2\right)\Big|_{\dot{\gamma}_R} = \frac{F_z}{\pi R^2}\left[2 + \frac{d\ln(F_z)}{d\ln\dot{\gamma}_R} \right]}$$

(Not a direct material funcion)

Macosko, Rheology: *Principles, Measurements, and Applications*, VCH 1994, p220

49

© Faith A. Morrison, Michigan Tech U.

Torsional Cone and Plate

(spherical coordinates)

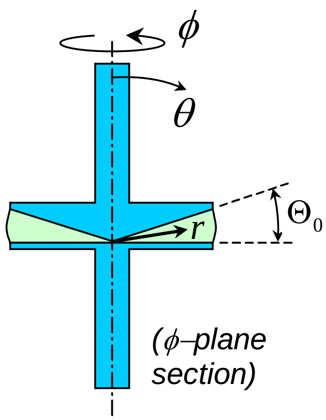

$$\underline{v} = \begin{pmatrix} 0 \\ 0 \\ v_\phi(r,\theta) \end{pmatrix}_{r\theta\phi}$$

50

© Faith A. Morrison, Michigan Tech U.

To calculate shear rate:

$$\underline{v} = \begin{pmatrix} 0 \\ 0 \\ A(-r\theta)+B \end{pmatrix}_{r\theta\phi}$$

$$v_\phi = A(-r\theta) + B$$

$$v_\phi = \frac{r\Omega}{\Theta_0}\left(\frac{\pi}{2} - \theta\right)$$ (due to boundary conditions)

$$\dot{\gamma} = \left|\underline{\underline{\dot{\gamma}}}\right| = \left| \begin{pmatrix} 0 & 0 & r\frac{\partial}{\partial r}\left(\frac{v_\phi}{r}\right) \\ 0 & 0 & \frac{\sin\theta}{r}\frac{\partial}{\partial\theta}\left(\frac{v_\phi}{\sin\theta}\right) \\ r\frac{\partial}{\partial r}\left(\frac{v_\phi}{r}\right) & \frac{\sin\theta}{r}\frac{\partial}{\partial\theta}\left(\frac{v_\phi}{\sin\theta}\right) & 0 \end{pmatrix}_{r\theta\phi} \right|$$

$$\dot{\gamma} = ?$$

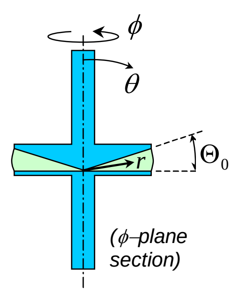

51

© Faith A. Morrison, Michigan Tech U.

Result: $\underline{v} = \begin{pmatrix} 0 \\ 0 \\ \frac{r\Omega}{\Theta_0}\left(\frac{\pi}{2} - \theta\right) \end{pmatrix}_{r\theta\phi}$ $\dot{\gamma} = \frac{\Omega}{\Theta_0} =$ constant

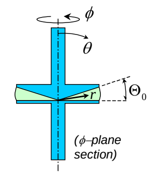

Note: The shear rate is a constant.

The extra stresses τ_{ij} are only a function of the shear rate, thus the τ_{ij} are constant as well.

$$\underline{\underline{\tau}} = \begin{pmatrix} \tau_{rr} & 0 & 0 \\ 0 & \tau_{\theta\theta} & \tau_{\theta\phi} \\ 0 & \tau_{\phi\theta} & \tau_{\phi\phi} \end{pmatrix}_{r\theta\phi}$$

(viscometric flow)

Result: $\tau_{ij} =$ constant

Torsional cone and plate is a homogeneous shear flow.

Assume:
- Form of velocity
- no ϕ-dependence
- no slip
- isothermal

52

© Faith A. Morrison, Michigan Tech U.

Result: $\tau_{\theta\phi} = C$

The experimentally measurable variable is the torque to turn the cone:

$$\underline{T} = \iint_S \left[\underline{R} \times \left(\hat{n} \cdot -\underline{\underline{\Pi}}\right)\right]_{surface} dS$$

$$\underline{T} = \int_0^{2\pi}\int_0^{R} \left[r\hat{e}_r \times \left(-\hat{e}_\theta \cdot -\underline{\underline{\Pi}}\right)\right]_{\theta=\frac{\pi}{2}} r dr d\phi$$

$$T_\theta = T_z = \frac{2\pi R^3 \tau_{\theta\phi}}{3}$$

For an arbitrary fluid, we are able to relate the torque and the shear stress.

53

© Faith A. Morrison, Michigan Tech U.

Torsional Cone-and-Plate Flow - Viscosity

Measureables:
Torque **T** to turn cone
Rate of angular rotation Ω

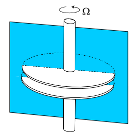

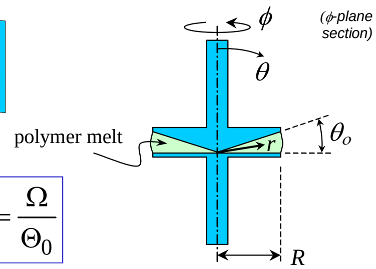

The introduction of the cone means that shear rate is independent of r.

$$\boxed{\dot{\gamma} = \frac{\Omega}{\Theta_0}}$$

Since shear rate is constant everywhere, so is extra stress, and we can calculate stress from torque.

$$\boxed{\tau_{\theta\phi} = \text{constant} = \frac{3T}{2\pi R^3}}$$

$$\boxed{\eta(\dot{\gamma}) = \frac{3T\Theta_0}{2\pi R^3 \Omega}}$$

No corrections needed in cone-and-plate

(and no material assumptions)

54

© Faith A. Morrison, Michigan Tech U.

To calculate normal stresses, look at EOM:

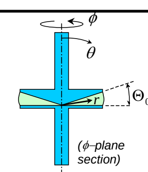

$$P \equiv p - \rho g z$$

$$\rho\left(\cancel{\frac{\partial \underline{v}}{\partial t}} + \cancel{\underline{v}\cdot\nabla\underline{v}}\right) = -\nabla P - \nabla\cdot\underline{\underline{\tau}}$$

steady state

neglect inertia

Also, the pressure is not constant

Although the stress is constant, there are some non-zero terms in the divergence of the stress in the $r\theta\phi$ coordinate system

$$\underline{\underline{\tau}} = \begin{pmatrix} \tau_{rr} & 0 & 0 \\ 0 & \tau_{\theta\theta} & \tau_{\theta\phi} \\ 0 & \tau_{\phi\theta} & \tau_{\phi\phi} \end{pmatrix}_{r\theta\phi}$$

(viscometric flow)

$$\begin{pmatrix} 0 \\ 0 \\ 0 \end{pmatrix}_{r\theta\phi} = \begin{pmatrix} -\frac{\partial P}{\partial r} \\ -\frac{1}{r}\frac{\partial P}{\partial \theta} \\ 0 \end{pmatrix}_{r\theta\phi} - \begin{pmatrix} \frac{1}{r^2}\frac{\partial r^2 \tau_{rr}}{\partial r} - \frac{\tau_{\theta\theta} + \tau_{\phi\phi}}{r} \\ \frac{1}{r\sin\theta}\frac{\partial \tau_{\theta\theta}\sin\theta}{\partial\theta} - \frac{\tau_{\phi\phi}\cot\theta}{r} \\ \frac{1}{r\sin\theta}\frac{\partial \tau_{\theta\phi}\sin\theta}{\partial\theta} + \frac{\tau_{\phi\theta}\cot\theta}{r} \end{pmatrix}_{r\theta\phi}$$

Assume:
- Form of velocity
- no ϕ-dependence
- symmetric stress tensor
- neglect inertia
- no slip
- isothermal

55

© Faith A. Morrison, Michigan Tech U.

On the bottom plate, *sin*θ=1, *cos*θ=0:

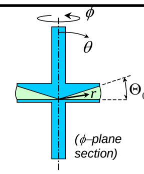

$$\begin{pmatrix} 0 \\ 0 \\ 0 \end{pmatrix}_{r\theta\phi} = \begin{pmatrix} -\frac{\partial P}{\partial r} \\ -\frac{1}{r}\frac{\partial P}{\partial \theta} \\ 0 \end{pmatrix}_{r\theta\phi} - \begin{pmatrix} \frac{2\tau_{rr}}{r} - \frac{\tau_{\theta\theta}+\tau_{\phi\phi}}{r} \\ 0 \\ 0 \end{pmatrix}_{r\theta\phi}$$

$$0 = -\frac{\partial P}{\partial r} - \frac{2\tau_{rr}}{r} + \frac{\tau_{\theta\theta}+\tau_{\phi\phi}}{r}$$

$$0 = -\frac{\partial (P+\tau_{\theta\theta})}{\partial r} - \frac{2\tau_{rr}}{r} + \frac{\tau_{\theta\theta}+\tau_{\phi\phi}}{r}$$

(valid to insert, since extra stress is constant)

$$-\Psi_1\dot{\gamma}_0^2 = \tau_{\phi\phi} - \tau_{\theta\theta}$$
$$-\Psi_2\dot{\gamma}_0^2 = \tau_{\theta\theta} - \tau_{rr}$$

(by definition)

$$\boxed{\frac{\partial \Pi_{\theta\theta}}{\partial \ln r} = -\dot{\gamma}_0^2\left(\Psi_1 + 2\Psi_2\right)}$$

56

© Faith A. Morrison, Michigan Tech U.

Result: $$\boxed{\frac{\partial \Pi_{\theta\theta}}{\partial \ln r} = -\dot{\gamma}_0^2\left(\Psi_1 + 2\Psi_2\right)}$$

The experimentally measurable variable is the fluid thrust on the plate minus the thrust of P_{atm}:

$$N = F_z - \pi R^2 P_{atm}$$

$$\underline{F} = \iint_S \left[\left(\hat{n}\cdot -\underline{\underline{\Pi}}\right)\right]_{surface} dS$$

$$\underline{F} = \int_0^{2\pi}\int_0^R \left[\left(-\hat{e}_\theta \cdot -\underline{\underline{\Pi}}\right)\right]_{\theta=\frac{\pi}{2}} r dr d\phi$$

$$F_\theta = F_z = 2\pi \int_0^R \Pi_{\theta\theta}\Big|_{\theta=\frac{\pi}{2}} r dr$$

57

© Faith A. Morrison, Michigan Tech U.

Integrate:

$$\frac{\partial \Pi_{\theta\theta}}{\partial \ln r} = -\dot{\gamma}_0^2\left(\Psi_1 + 2\Psi_2\right)$$

$$\Pi_{\theta\theta} = -\dot{\gamma}_0^2\left(\Psi_1 + 2\Psi_2\right)\ln r + C$$

Boundary condition:

$$r = R$$

$$\Pi_{\theta\theta} = P_{atm} + \tau_{\theta\theta}\big|_R$$

$$= P_{atm} \underbrace{- \Psi_2\dot{\gamma}_0^2 + \tau_{RR}}_{\text{Directly from definition of } \Psi_2}$$

$$\Pi_{\theta\theta} = -\dot{\gamma}_0^2\left(\Psi_1 + 2\Psi_2\right)\ln\frac{r}{R} + P_{atm} - \Psi_2\dot{\gamma}_0^2$$

$$N = F_z - \pi R^2 P_{atm}$$

$$N = 2\pi\int_0^R \Pi_{\theta\theta}\big|_{\theta=\frac{\pi}{2}} r\,dr - -\pi R^2 P_{atm}$$

. . .

58

© Faith A. Morrison, Michigan Tech U.

Torsional Cone-and-Plate Flow – 1st Normal Stress

Measureables:
Normal thrust **F**

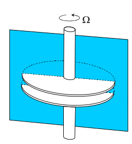

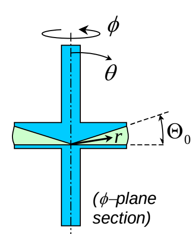

$$N = \left[2\pi\int_0^R \Pi_{\theta\theta}\big|_{\theta=\frac{\pi}{2}} r\,dr\right] - \pi R^2 p_{atm}$$

The total upward thrust of the cone can be related directly to the first normal stress coefficient.

$$\boxed{\Psi_1(\dot{\gamma}) = \frac{2F\Theta_0^2}{\pi R^2\Omega^2}}$$

(see also DPL pp522)

59

© Faith A. Morrison, Michigan Tech U.

Torsional Cone-and-Plate Flow – 2nd Normal Stress

$$\Pi_{\theta\theta} = -\dot{\gamma}_0^2\left(\Psi_1 + 2\Psi_2\right)\ln\frac{r}{R} + P_{atm} - \Psi_2\dot{\gamma}_0^2$$

If we obtain $\Pi_{\theta\theta}$ as a function of r / R, we can also obtain Ψ_2.

•MEMS used to manufacture sensors at different radial positions

The Normal Stress Sensor System (NSS)

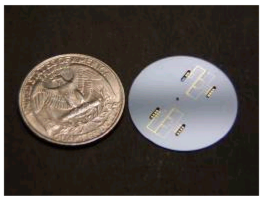

Patented Technology

RheoSense Incorporated
(www.rheosense.com)

•S. G. Baek and J. J. Magda, J. Rheology, 47(5), 1249-1260 (2003)
•J. Magda et al. Proc. XIV International Congress on Rheology, Seoul, 2004.

60

© Faith A. Morrison, Michigan Tech U.

RheoSense Incorporated

Comparison with other instruments

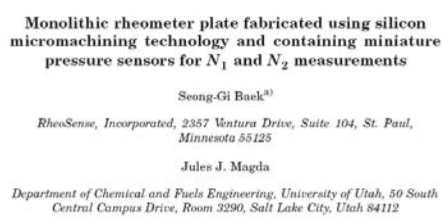

Monolithic rheometer plate fabricated using silicon micromachining technology and containing miniature pressure sensors for N_1 and N_2 measurements

Seong-Gi Baek[a]

RheoSense, Incorporated, 2357 Ventura Drive, Suite 104, St. Paul, Minnesota 55125

Jules J. Magda

Department of Chemical and Fuels Engineering, University of Utah, 50 South Central Campus Drive, Room 3290, Salt Lake City, Utah 84112

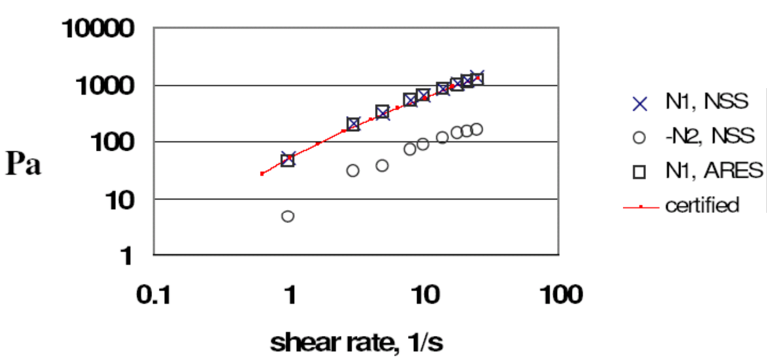

S. G. Baek and J. J. Magda, J. Rheology, 47(5), 1249-1260 (2003)

61

© Faith A. Morrison, Michigan Tech U.

Treated in detail in Macosko, pp 188-205

Couette Flow (1890)

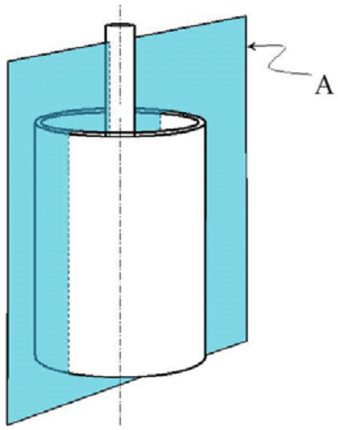

- •Tangential annular flow
- •Cup and Bob geometry

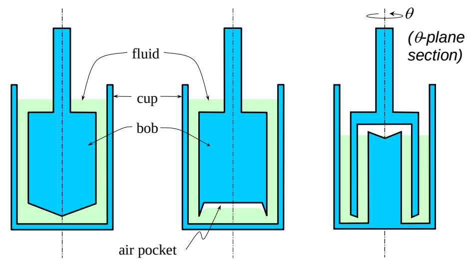

Assume:
- •Form of velocity
- •no θ-dependence
- •symmetric stress tensor
- •Neglect gravity
- •Neglect end effects
- •no slip
- •isothermal

Macosko, Rheology: *Principles, Measurements, and Applications*, VCH 1994.

62

© Faith A. Morrison, Michigan Tech U.

Couette Flow

Assume:
- •Form of velocity
- •no θ-dependence
- •symmetric stress tensor
- •Neglect gravity
- •Neglect end effects
- •no slip
- •isothermal

$$\eta = \frac{T(\kappa - 1)}{2\pi R^2 L \kappa^3 \Omega}$$

$$\kappa = \frac{R_{inner}}{R_{outer}}$$

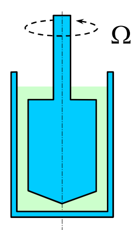

As with many measurement systems, the assumptions made in the analysis do not always hold:

- •End effects are not negligible
- •Wall slip occurs with many systems
- •Inertia is not always negligible
- •Secondary flows occur (cup turning is more stable than bob turning to inertial instabilities; there are elastic instabilities; there are viscous heating instabilities)
- •Alignment is important
- •Viscous heating occurs
- •Methods for measuring Ψ_1 are error prone
- •Cannot measure Ψ_2

BUT
- •Generates a lot of signal
- •Can go to high shear rates
- •Is widely available
- •Is well understood

Macosko, Rheology: *Principles, Measurements, and Applications*, VCH 1994.

63

© Faith A. Morrison, Michigan Tech U.

For the PP and CP geometries, we can also calculate *G′, G″*:

Parallel plate

$$\eta'(\omega) = \frac{G''(\omega)}{\omega} = \frac{2HT_0 \sin\delta}{\pi R^4 \omega \theta_0}$$

$$\eta''(\omega) = \frac{G'(\omega)}{\omega} = \frac{2HT_0 \cos\delta}{\pi R^4 \omega \theta_0}$$

Amplitude of oscillation

Cone and plate

$$\eta'(\omega) = \frac{3\Theta_0 T_0 \sin\delta}{2\pi R^3 \omega \phi_0}$$

$$\eta''(\omega) = \frac{3\Theta_0 T_0 \cos\delta}{2\pi R^3 \omega \phi_0}$$

Amplitude of oscillation

- A typical diameter is between 8 and 25mm; 30-40mm are also used
- To increase accuracy, larger plates (R larger) are used for less viscous materials to generate more torque.
- Amplitude may also be increased to increase torque
- A complete analysis of SAOS in the Couette geometry is given in Sections 8.4.2-3

© Faith A. Morrison, Michigan Tech U.

Limits on Measurements: Flow instabilities in rheology

Cone and plate/Parallel plate flow

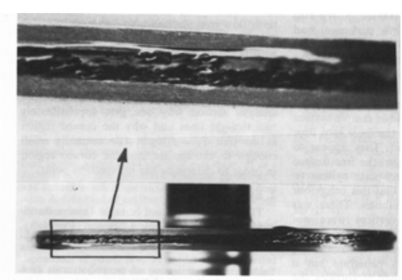

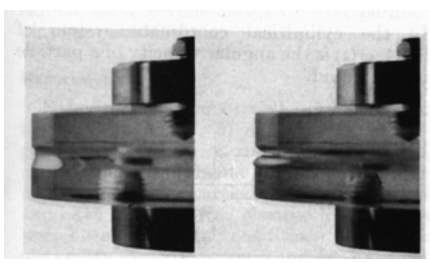

Figures 6.7 and 6.8, p. 175 Hutton; PDMS

© Faith A. Morrison, Michigan Tech U.

Taylor-Couette flow

1923 GI Taylor; inertial instability
1990 Ron Larson, Eric Shaqfeh, Susan Muller; elastic instability

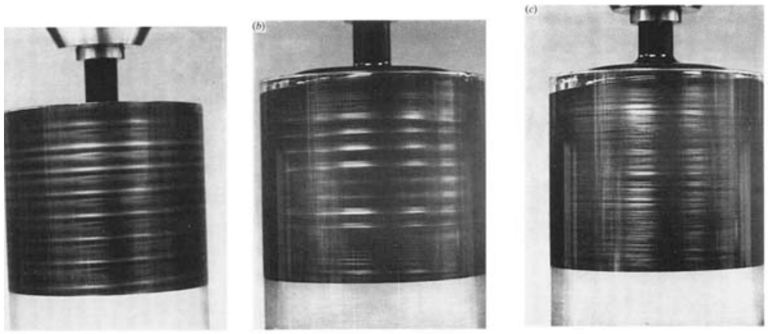

FIGURE 11. Flow visualizations in a Taylor-Couette cell. (*a*) Newtonian fluid at high Taylor number ($Ta = 3800$); (*b*) Boger fluid at negligible Taylor number ($Ta = 9.6 \times 10^{-8}$) shortly after the onset of secondary flow (t_2 in figure 9); (*c*) Boger fluid at negligible Taylor number after full development of secondary flow (t_3 in figure 9).

•GI Taylor "Stability of a viscous liquid contained between two rotating cylinders," *Phil. Trans. R. Soc. Lond*. A 223, 289 (1923)
•Larson, Shaqfeh, Muller, "A purely elastic instability in Taylor-Couette flow,"*J. Fluid Mech*, 218, 573 (1990)

© Faith A. Morrison, Michigan Tech U.

Why do we need more than one method of measuring viscosity?

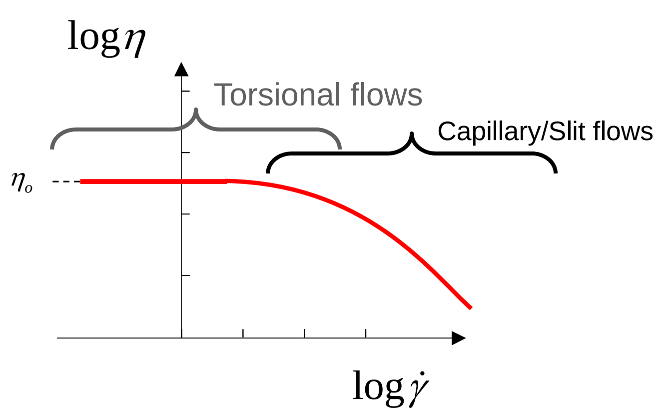

•At low rates, torques/pressures become low
•At high rates, torques/pressures become high; flow instabilities set in

© Faith A. Morrison, Michigan Tech U.

Shear measurement
Material Function Calculations

TABLE 10.2
Summary of the Expressions for Steady Shear Rheological Quantities for Common Geometries*

Geometry	Magnitude of Shear Stress $\lvert\tau_{21}\rvert$	Shear Rate $\dot{\gamma}$	Measured Material Function
Capillary flow (wall conditions) $\mathcal{P}_0, \mathcal{P}_L$ = modified pressure at $z = 0, L$ Q = flow rate L = capillary length $\mathcal{R} = \frac{1}{4}\left[3 + \frac{d\ln(4Q/\pi R^3)}{d\ln\tau_R}\right]$ $\tau_R = \tau_{rz}\vert_{r=R}$	$\frac{(\mathcal{P}_0 - \mathcal{P}_L)R}{2L}$	$\frac{4Q}{\pi R^3}\mathcal{R}$	$\eta = \frac{\tau_R}{4Q/\pi R^3}\mathcal{R}^{-1}$
Parallel disk (at rim) $\mathcal{T}$ = torque on top plate Ω = angular velocity of top plate, > 0 H = gap $\mathcal{R} = \frac{1}{4}\left[3 + \frac{d\ln(\mathcal{T}/2\pi R^3)}{d\ln\dot{\gamma}_R}\right]$ $\dot{\gamma}_R = \dot{\gamma}(R)$	$\frac{2\mathcal{T}}{\pi R^3}\mathcal{R}$	$\frac{r\Omega}{H}$	$\eta = \frac{2\mathcal{T}}{\pi R^3\dot{\gamma}_R}\mathcal{R}$
Cone and plate $\mathcal{T}$ = torque on plate $\mathcal{F}$ = thrust on plate Ω = angular velocity of cone, > 0 Θ_0 = cone angle	$\frac{3\mathcal{T}}{2\pi R^3}$	$\frac{\Omega}{\Theta_0}$	$\eta = \frac{3\mathcal{T}\Theta_0}{2\pi R^3\Omega}$ $\Psi_1 = \frac{2\mathcal{F}\Theta_0^2}{\pi R^2\Omega^2}$
Couette (bob turning) $\mathcal{T}$ = torque on inner cylinder, < 0 Ω = angular velocity of bob, > 0 R = outer radius κR = inner radius L = length of bob	$\frac{-\mathcal{T}}{2\pi R^2 L\kappa^2}$	$\frac{\kappa\Omega}{1-\kappa}$	$\eta = \frac{\mathcal{T}(\kappa - 1)}{2\pi R^2 L\kappa^3\Omega}$
Couette (cup turning) $\mathcal{T}$ = torque on inner cylinder, > 0 Ω = angular velocity of cup, > 0 R = outer radius κR = inner radius L = length of bob	$\frac{\mathcal{T}}{2\pi R^2 L\kappa^2}$	$\frac{\kappa\Omega}{1-\kappa}$	$\eta = \frac{\mathcal{T}(1-\kappa)}{2\pi R^2 L\kappa^3\Omega}$

* R is radius of fixture. To calculate strain in each case, multiply shear rate by time t. Note that $\eta \equiv -\tau_{21}/\dot{\gamma}_0 = \lvert\tau_{21}\rvert/\dot{\gamma}$.

See also Macosko, Part II

© Faith A. Morrison, Michigan Tech U.

Shear measurements
Pros and Cons

TABLE 10.3
Comparison of Experimental Features of Four Common Shear Geometries

Feature	Parallel Disk	Cone and Plate	Capillary	Couette (Cup and Bob)
Stress range	Good for high viscosity	Good for high viscosity	Good for high viscosities	Good for low viscosities
Flow stability	Edge fracture at modest rates	Edge fracture at modest rates	Melt fracture at very high rates, i.e., distorted extrudates and pressure fluctuations are observed	Taylor cells are observed at high Re due to inertia; elastic cells are observed at high De
Sample size and sample loading	< 1 g; easy to load	< 1 g; highly viscous materials can be difficult to load	40 g minimum; easy to load	10–20 g; highly viscous materials can be difficult to load
Data handling	Correction on shear rate needs to be applied; this correction is ignored in most commercial software packages	Straightforward	Multiple corrections need to be applied	Straightforward
Homogeneous?	No; shear rate and shear stress vary with radius	Yes (small core angles)	No; shear rate and shear stress vary with radius	Yes (narrow gap)
Pressure effects	None	None	High pressures in reservoir cause problems with compressibility of melt	None
Shear rates	Maximum shear rate is limited by edge fracture; usually cannot obtain shear-thinning data	Maximum shear rate is limited by edge fracture; usually cannot obtain shear-thinning data	Very high rates accessible	Maximum shear rate is limited by sample leaving cup due to either inertia or elastic effects; also 3-D secondary flows develop (instability)
Special features	Good for stiff samples, even gels; wide range of temperatures possible	Ψ_1 measurable; wide range of temperatures possible	Constant-Q or constant-$\Delta\mathcal{P}$ modes available; wide range of temperatures possible	Narrow gap required; usually limited to modest temperatures (e.g., $0 < T < 60°C$)

69

© Faith A. Morrison, Michigan Tech U.

Stress/Strain Driven Drag
Multipurpose rheometers

TA Instruments
Anton Paar
Malvern
Thermo Scientific
Brookfield
ATS RheoSystems

Pressure-driven Shear

Göttfert
Instron
ATS RheoSystems
Malvern

(capillary, slit flow; melts)

RheoSense, Inc.

(Slit flow; microfluidics)

Optical

LS Instruments

(diffusive wave spectroscopy; G'G")

(plus attachments on multipurpose rheometer)

Interfacial Rheology

Anton Paar
TA Instruments
BiolinScientific

(drag flow on interface)

70

© Faith A. Morrison, Michigan Tech U.

Elongational Flow Measurements

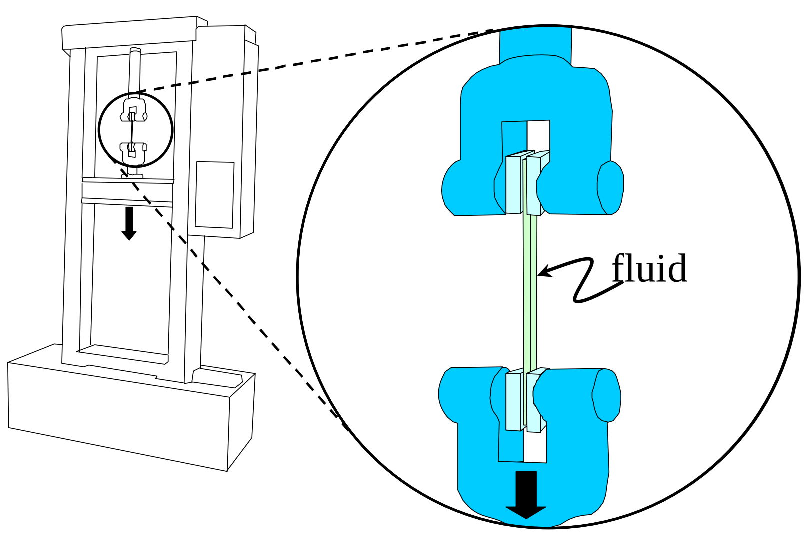

71

© Faith A. Morrison, Michigan Tech U.

Experimental Elongational Geometries

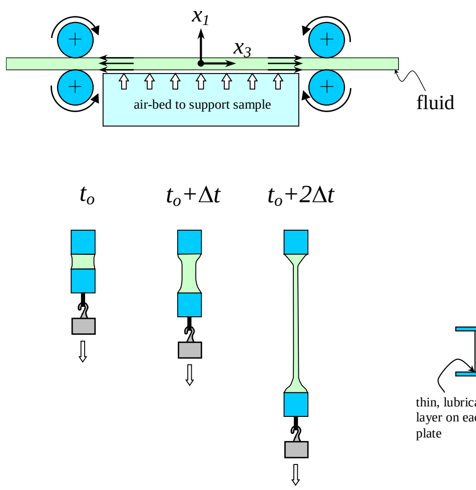

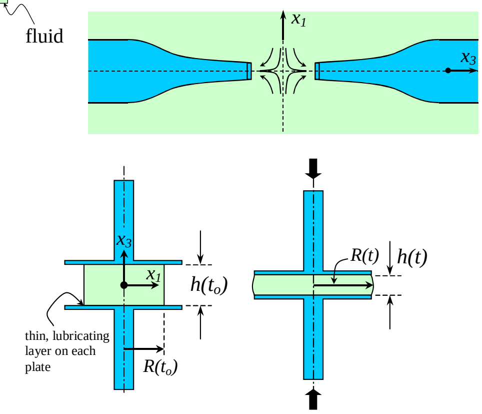

72

© Faith A. Morrison, Michigan Tech U.

Uniaxial Extension

tensile force

$$\tau_{zz} - \tau_{rr} = -\frac{f(t)}{A(t)}$$

time-dependent cross-sectional area

For homogeneous flow: $A(t) = A_0 e^{-\dot{\varepsilon}_0 t}$

$$\boxed{\bar{\eta} = \frac{-(\tau_{zz} - \tau_{rr})}{\dot{\varepsilon}_0} = \frac{f(t_\infty) e^{\dot{\varepsilon}_0 t_\infty}}{A_0 \dot{\varepsilon}_0}}$$

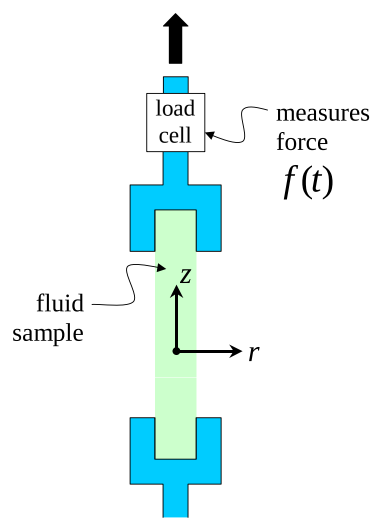

73

© Faith A. Morrison, Michigan Tech U.

Experimental Difficulties in Elongational Flow

ideal elongational deformation

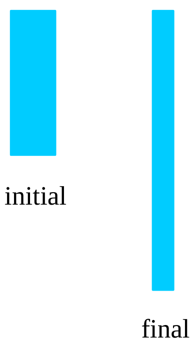

experimental challenges

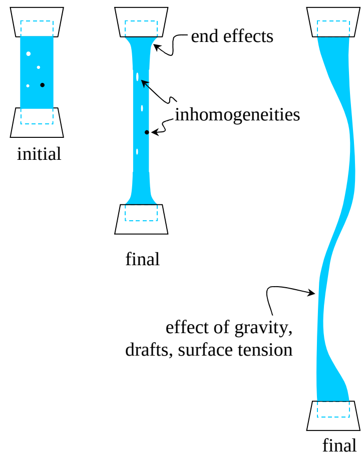

74

© Faith A. Morrison, Michigan Tech U.

Filament Stretching Rheometer (FiSER)

Tirtaatmadja and Sridhar, J. Rheol., 37, 1081-1102 (1993)

- •Optically monitor the midpoint size
- •Very susceptible to environment
- •End Effects

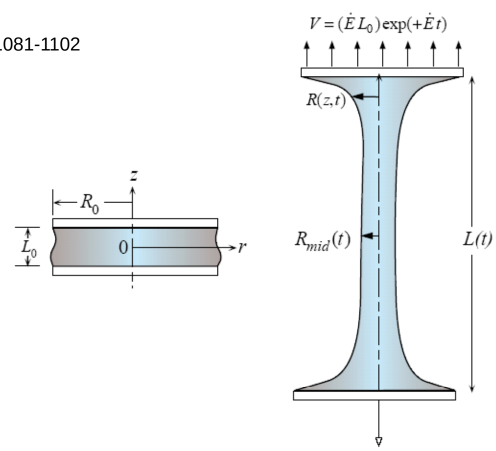

McKinley, et al., 15th Annual Meeting of the International Polymer Processing Society, June 1999.

75

© Faith A. Morrison, Michigan Tech U.

Filament Stretching Rheometer

(Design based on Tirtaatmadja and Sridhar)

"The test sample (a) undergoing investigation is placed between two parallel, circular discs (b) and (c) with diameter $2R_0$=9 mm. The upper disc is attached to a movable sled (d), while the lower disc is in contact with a weight cell (e). The upper sled is driven by a motor (f), which also drives a mid-sled placed between the upper sled and the weight cell; two timing belts (g) are used for transferring momentum from the motor to the sleds. The two toothed wheels (h), driving the timing belts have a 1:2 diameter ratio, ensuring that the mid-sled always drives at half the speed of the upper sled. This means that if the mid-sled is placed in the middle between the upper and the lower disc at the beginning of an experiment, it will always stay midway between the discs. On the mid-sled, a laser (i) is placed for measuring the diameter of the mid-filament at all times.

Bach, Rasmussen, Longin, Hassager, JNNFM 108, 163 (2002)

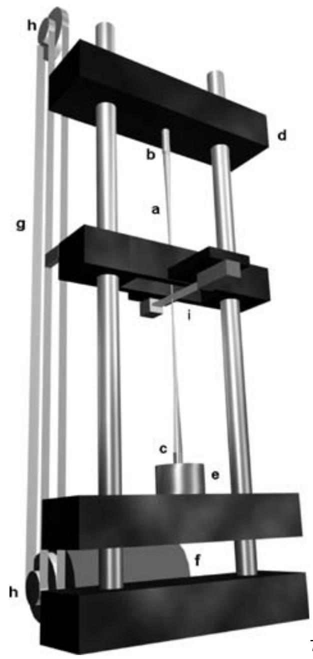

© Faith A. Morrison, Michigan Tech U.

Rheol Acta (2001) 40: 457–466
© Springer-Verlag 2001
ORIGINAL CONTRIBUTION

Jonathan S. Schulze
Timothy P. Lodge
Christopher W. Macosko
Jens Hepperle
Helmut Münstedt
Heike Bastian
Dino Ferri
David J. Groves
Yong Hoon Kim
Mike Lyon
Thomas Schweizer
Terry Virkler
Erik Wassner
Wim Zoetelief

A comparison of extensional viscosity measurements from various RME rheometers

- Steady and startup flow
- Recovery
- Good for melts

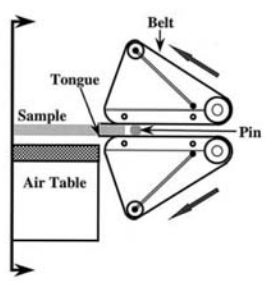

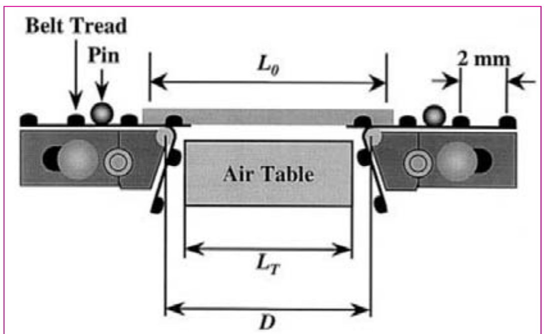

RHEOMETRICS RME 1996 (out of production)

© Faith A. Morrison, Michigan Tech U.

Conclusions

Extensional viscosity measurements of a slightly strain hardening LLDPE (Dow Affinity PL 1880) from several Rheometric Scientific RME extensional rheometers were compared with data obtained from the original version of the RME at the ETH Institut für Polymere in Zürich and the Münstedt Tensile Rheometer (MTR) at the University of Erlangen. In general, the commercial RMEs extended samples with a strain rate that was significantly less than the set strain rate. The problem worsened at the higher strain rates of 1.0 s^{-1} and 0.1 s^{-1}, where the difference was at least 10%. The data from the commercial RMEs typically agree with the MTR and original RME within 20%, after the extensional viscosity is corrected for the strain rate.

Achieving commanded strain requires great care.

increased from 50 mm to 60 mm, the deviation in the strain rate decreased from 20% to 2–6%. The recommended value of L_0 should be determined by measuring the distance D and using Eq. (4). However, operating the RME with the correct value of L_0 does not eliminate entirely the strain rate deviation. Based on the performance of earlier rotary clamp rheometers, the strain rate deviation most likely occurs because the velocity of the belts is not sufficiently transferred to the sample during the test. Clearly, the deformation of all materials must be monitored with a video camera, and analyzed to obtain the true strain rate applied to the sample during the test.

Use of the video camera (although tedious) is recommended in order to get correct strain rate.

78

© Faith A. Morrison, Michigan Tech U.

Sentmanat Extension Rheometer (2005)

- Originally developed for rubbers, good for melts
- Measures elongational viscosity, startup, other material functions
- Two counter-rotating drums
- Easy to load; reproducible

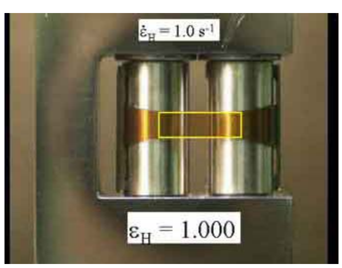

www.xpansioninstruments.com

http://www.xpansioninstruments.com/rheo-optics.htm

79

© Faith A. Morrison, Michigan Tech U.

Sentmanat et al., J. Rheol., 49(3) 585 (2005)

Comparison on different host instruments

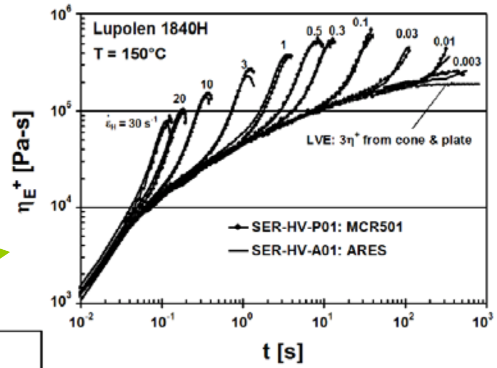

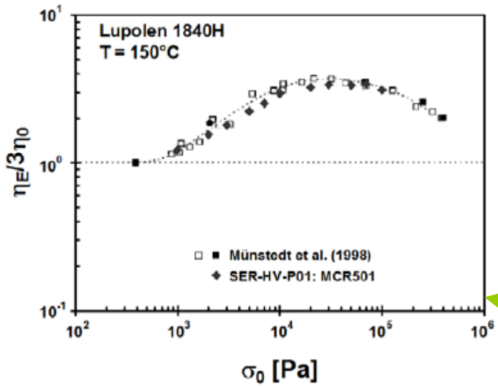

Comparison with other instruments (literature)

© Faith A. Morrison, Michigan Tech U.

CaBER Extensional Rheometer

- •Polymer solutions
- •Works on the principle of capillary filament break up
- •Cambridge Polymer Group and HAAKE

For more on theory see: campoly.com/notes/007.pdf

Brochure: www.thermo.com/com/cda/product/detail/1,,17848,00.html

Operation

- •Impose a rapid step elongation
- •form a fluid filament, which continues to deform
- •flow driven by surface tension
- •also affected by viscosity, elasticity, and mass transfer
- •measure midpoint diameter as a function of time
- •Use force balance on filament to back out an apparent elongational viscosity

© Faith A. Morrison, Michigan Tech U.

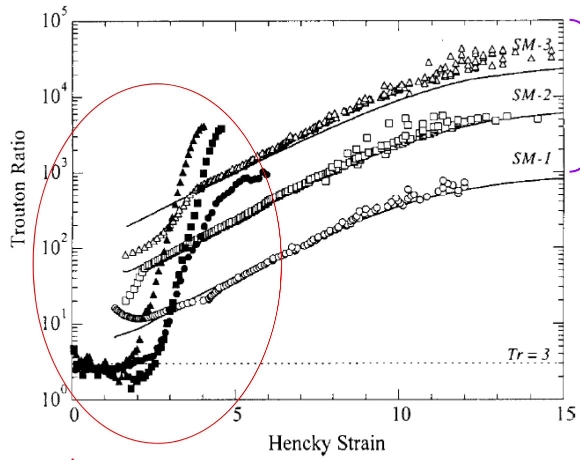

Capillary breakup experiments

Comments

- Must know surface tension
- Transient agreement is poor
- Steady state agreement is acceptable
- Be aware of effect modeling assumptions on reported results

Filament stretching apparatus

Anna and McKinley, J. Rheol. 45, 115 (2001).

82

© Faith A. Morrison, Michigan Tech U.

Elongational Viscosity via Contraction Flow: Cogswell/Binding Analysis

Fluid elements along the centerline undergo considerable elongational flow

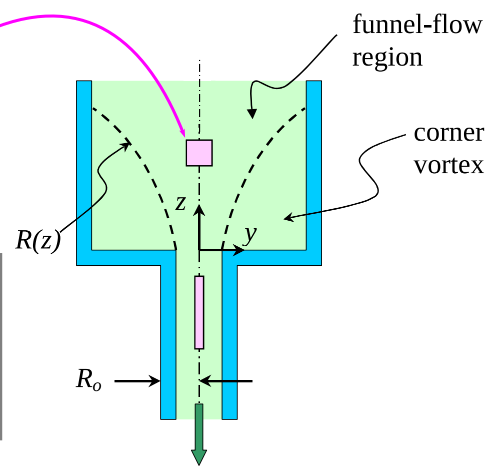

By making strong assumptions about the flow we can relate the pressure drop across the contraction to an elongational viscosity

83

© Faith A. Morrison, Michigan Tech U.

This flow is produced in some capillary rheometers:

$$\frac{P_{reservoir} - P_{atm}}{L} = \frac{\Delta P_{entrance}}{L} + \frac{\Delta P_{true}}{L}$$

We can use this "discarded" measurement to rank elongational properties

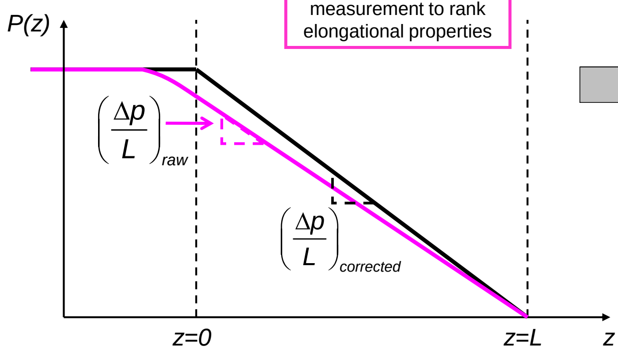

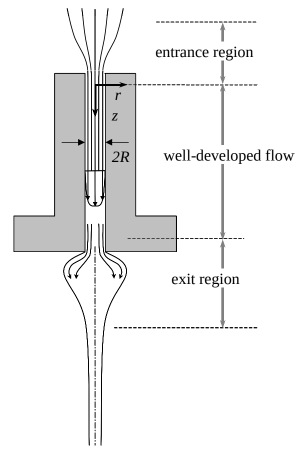

84

© Faith A. Morrison, Michigan Tech U.

Bagley Plot

$$\Delta P_{\substack{end\\effects}} = f(Q) = f(\dot{\gamma}_a)$$

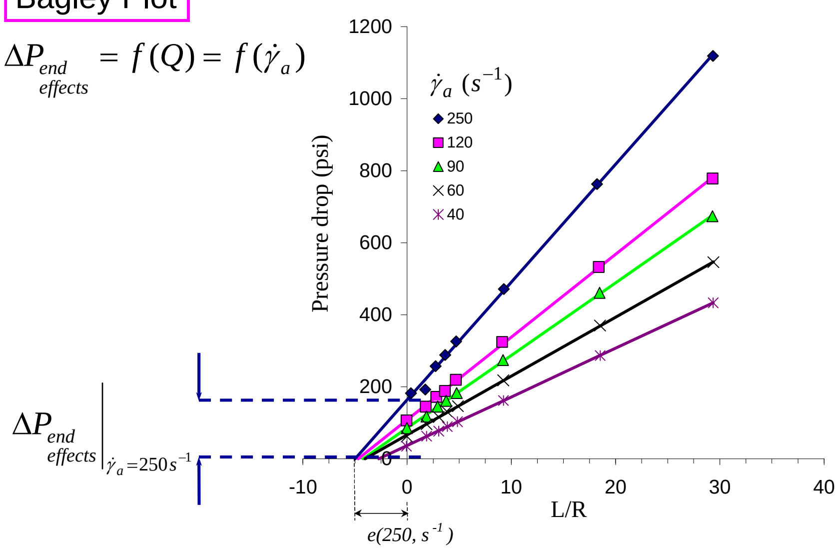

Figure 10.8, p. 394 Bagley, PE

85

© Faith A. Morrison, Michigan Tech U.

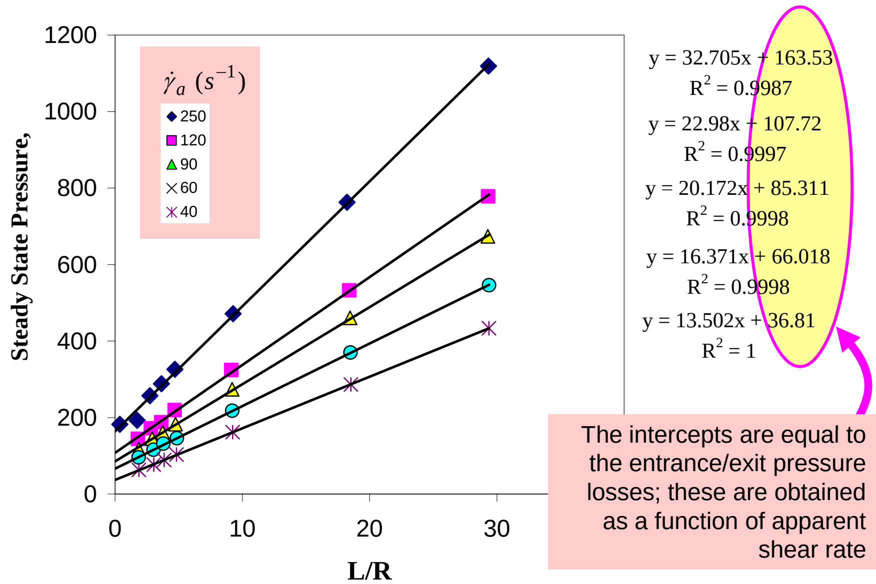

The intercepts are equal to the entrance/exit pressure losses; these are obtained as a function of apparent shear rate

Figure 10.8, p. 394 Bagley, PE

86

© Faith A. Morrison, Michigan Tech U.

Assumptions for the Cogswell Analysis

- incompressible fluid
- funnel-shaped flow; no-slip on funnel surface
- unidirectional flow in the funnel region
- well developed flow upstream and downstream
- θ-symmetry
- pressure drops due to shear and elongation may be calculated separately and summed to give the total entrance pressure-loss
- neglect Weissenberg-Rabinowitsch correction
- shear stress is related to shear-rate through a power-law
- elongational viscosity is constant
- shape of the funnel is determined by the minimum generated pressure drop
- no effect of elasticity (shear normal stresses neglected)
- neglect inertia

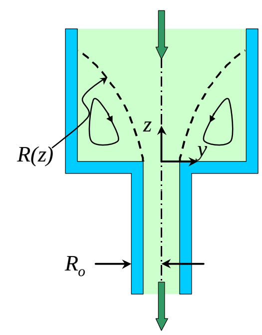

$$\dot{\gamma} \approx \dot{\gamma}_a$$
$$\underline{\tau_R} = m\dot{\gamma}_a^n$$
$$\eta = \text{constant}$$

F. N. Cogswell, Polym. Eng. Sci. (1972) 12, 64-73.
F. N. Cogswell, Trans. Soc. Rheol. (1972) 16, 383-403.

87

© Faith A. Morrison, Michigan Tech U.

Cogswell Analysis

elongation rate
$$\dot{\varepsilon}_o = \frac{\tau_R \dot{\gamma}_a}{2(\tau_{11} - \tau_{22})}$$

$$\tau_R = \eta\, \dot{\gamma}_a \qquad \dot{\gamma}_a = \frac{4Q}{\pi R^3} \qquad \eta = m \dot{\gamma}_a^{n-1}$$

elongation normal stress
$$(\tau_{11} - \tau_{22}) = -\frac{3}{8} \Delta p_{ent} \; (n+1)$$

elongation viscosity
$$\boxed{\bar{\eta} \approx \frac{-(\tau_{11} - \tau_{22})}{\dot{\varepsilon}_o} = \frac{\frac{9}{32}(n+1)^2 \Delta p_{ent}^2}{\tau_R \dot{\gamma}_a}}$$

© Faith A. Morrison, Michigan Tech U.

Cogswell Analysis – using Excel

From shear:
$$\eta = m \dot{\gamma}_a^{n-1}$$

(Binding's data)

$$\dot{\varepsilon}_o = \frac{\tau_R \dot{\gamma}_a}{2(\tau_{11} - \tau_{22})} \qquad \bar{\eta} = \frac{-(\tau_{11} - \tau_{22})}{\dot{\varepsilon}_o} \qquad 3\eta$$

$\dot{\gamma}_a = \frac{4Q}{\pi R^3}$ RAW DATA gammdotA	Δp_{ent} RAW DATA deltPent(psi)	Δp_{ent} deltPent(Pa)	τ_R sh stress(Pa)	N1(Pa)	e_rate	Cogswell elongvisc	Cogswell 3*shearVisc
250	163.53	1.13E+06	1.13E+05	-6.27E+05	2.25E+01	2.79E+04	1.55E+03
120	107.72	7.43E+05	7.92E+04	-4.13E+05	1.15E+01	3.59E+04	2.27E+03
90	85.311	5.88E+05	6.95E+04	-3.27E+05	9.56E+00	3.42E+04	2.65E+03
60	66.018	4.55E+05	5.64E+04	-2.53E+05	6.69E+00	3.79E+04	3.23E+03
40	36.81	2.54E+05	4.65E+04	-1.41E+05	6.59E+00	2.14E+04	4.00E+03

$$(\tau_{11} - \tau_{22}) = -\frac{3}{8} \Delta p_{ent} (n+1)$$

Results in one data point for elongational viscosity for each entrance pressure loss (i.e. each apparent shear rate)

© Faith A. Morrison, Michigan Tech U.

Assumptions for the Binding Analysis
- incompressible fluid
- funnel-shaped flow; no-slip on funnel surface
- unidirectional flow in the funnel region
- well developed flow upstream and downstream
- θ -symmetry
- shear viscosity is related to shear-rate through a power-law
- elongational viscosity is given by a power law
- shape of the funnel is determined by the minimum work to drive flow
- no effect of elasticity (shear normal stresses neglected)
- the quantities $(dR/dz)^2$ and d^2R/dz^2, related to the shape of the funnel, are neglected; implies that the radial velocity is neglected when calculating the rate of deformation
- neglect energy required to maintain the corner circulation
- neglect inertia

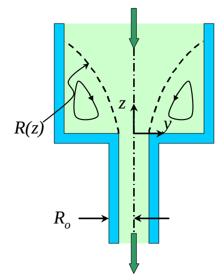

$$\tau_R = m\dot{\gamma}_a^n$$
$$\bar{\eta} = l\dot{\varepsilon}_o^{\,t-1}$$

D. M. Binding, JNNFM (1988) 27, 173-189.

90

© Faith A. Morrison, Michigan Tech U.

Binding Analysis

l, elongational prefactor

$$\Delta p_{ent} = \frac{2m(1+t)^2}{3t^2(1+n)^2}\left\{\frac{lt(3n+1)n^t I_{nt}}{m}\right\}^{1/(1+t)} \dot{\gamma}_{R_o}^{\,t(n+1)/(1+t)}\left\{1-\alpha^{3t(n+1)/(1+t)}\right\}$$

$$I_{nt} = \int_0^1 \left|2-\left(\frac{3n+1}{n}\right)\phi^{1+1/n}\right|^{t+1}\phi\,d\phi$$

$$\eta = m\dot{\gamma}_a^{n-1}$$

$$\dot{\gamma}_{R_o} = \frac{(3n+1)\,Q}{n\pi R_o^3}$$

$$\boxed{\text{elongation viscosity} \quad \eta = l\dot{\varepsilon}_o^{\,t-1}}$$

91

© Faith A. Morrison, Michigan Tech U.

Binding Analysis

Note: there is a non-iterative solution method described in the text; The method using Solver is preferable, since it uses all the data in finding optimal values of l and t.

Evaluation Procedure

1. Shear power-law parameter n must be known; must have data for Δp_{ent} versus Q
2. Guess t, l
3. Evaluate I_{nt} by numerical integration over ϕ
4. Using Solver, find the best values of t and l that are consistent with the Δp_{ent} versus Q data

Results in values of t, l for a model (power-law)

92

© Faith A. Morrison, Michigan Tech U.

Binding Analysis – using Excel Solver

$$I_{nt} = \int_0^1 \left| 2 - \left(\frac{3n+1}{n}\right)\phi^{1+1/n} \right|^{t+1} \phi \, d\phi$$

Evaluate integral numerically

phi	f(phi)	areas
0	0	
0.005	0.023746502	5.93663E-05
0.01	0.047492829	0.000178098
0.015	0.071238512	0.000296828
0.02	0.094982739	0.000415553
0.025	0.118724352	0.000534268
0.03	0.142461832	0.000652965
0.035	0.166193303	0.000771638
0.04	0.189916517	0.000890275
0.045	0.213628861	0.001008863
0.05	0.237327345	0.001127391
0.055	0.261008606	0.00124584
0.06	0.2846689	0.001364194
0.065	0.308304107	0.001482433

. . .

$$area = \frac{1}{2}(b_1 + b_2)h$$

Summing:

Int= 1.36055

93

© Faith A. Morrison, Michigan Tech U.

Binding Analysis – using Excel Solver

Optimize t, l using Solver

By varying these cells:

$$\frac{\left(predicted-actual\right)^2}{\left(actual\right)^2}$$

t_guess=	1.2477157	
l_guess=	11991.60895	
******* SOLVER SOLUTION ********		
predicted DeltaPent	exptal DeltaPent	difference
1.26E+06	1.13E+06	1.35E-02
6.88E+05	7.43E+05	5.51E-03
5.43E+05	5.88E+05	6.02E-03
3.89E+05	4.55E+05	2.14E-02
2.78E+05	2.54E+05	9.28E-03
	target cell	5.57E-02

Sum of the differences: Minimize this cell

94

© Faith A. Morrison, Michigan Tech U.

Example calculation from Bagley's Data

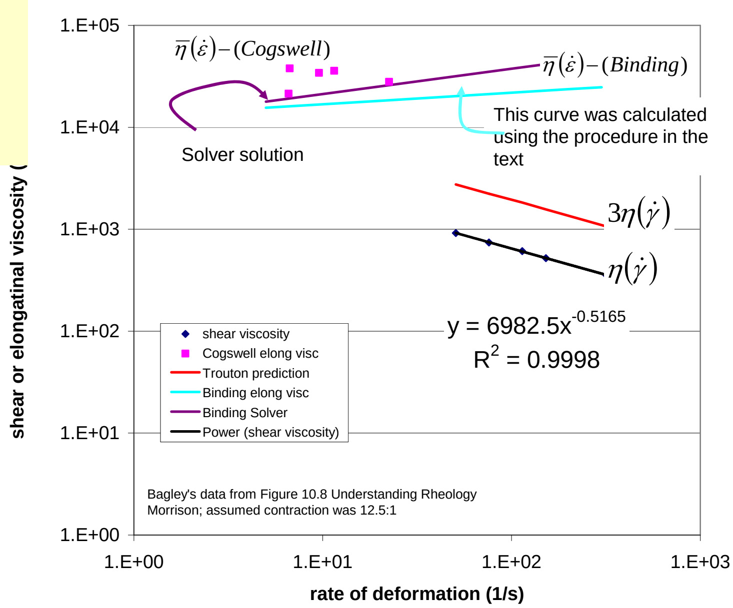

95

© Faith A. Morrison, Michigan Tech U.

Rheotens (Goettfert)

from their brochure:

"Rheotens test is a rather complicated function of the characteristics of the polymer, dimensions of the capillary, length of the spin line and of the extrusion history"

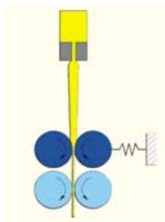

www.goettfert.com/downloads/Rheotens_eng.pdf

- Does not measure material functions without constitutive model
- small changes in material properties are reflected in curves
- easy to use
- excellent reproducibility
- models fiber spinning, film casting
- widespread application

96

© Faith A. Morrison, Michigan Tech U.

An elongational viscosity may be extracted from a "grand master curve" under some conditions

"The rheology of the rheotens test," M.H. Wagner, A. Bernnat, and V. Schulze, J. Rheol. 42, 917 (1998)

Raw data

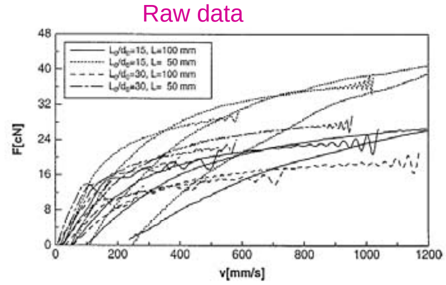

Grand master curve

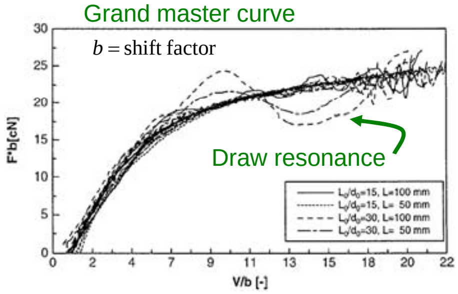

vs. draw ratio $V = v/v_{\text{die exit}}$

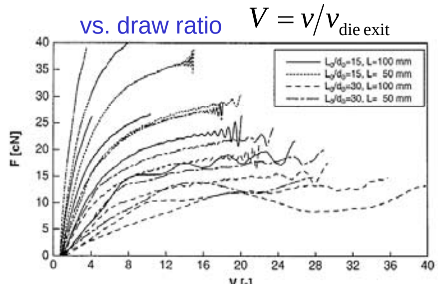

97

© Faith A. Morrison, Michigan Tech U.

Elongational measurements

Pros and Cons

TABLE 10.6
A Comparison of Experimental Features of Four Elongational Geometries

Feature	Melt Stretching	MBER	Filament Stretching	Binding/ Cogswell
Stress Range	Good for high viscosity	Good for high viscosity	Good for low viscosity at room temperature	Good for high and low viscosities
Flow stability	Subject to gravity, surface tension and air currents	Can be unstable at high rates	Subject to gravity, surface tension and air currents	Unstable at very high rates
Sample size and sample loading	10 g; care must be taken to minimize end effects	<2 g; requires careful preparation and loading	<1 g; easy to load	40 g minimum; easy to load
Data handling	Straightforward, but does not result in any elongational material functions	Straightforward; more involved if strain is measured	Two tests are required to account for strain inhomogeneities	Cogswell—straightforward Binding—more complicated but not difficult
Homogeneous?	No, not at ends	Could be with care	No, not at ends	No—mixed shear and elongational flow
Pressure effects	No	No	No	Yes—compressibility of melt reservoir could cause difficulties
Elongation rates	Maximum rates depend on clamp speeds	Maximum elongation rate is limited by ability to maintain the sample in steady flow	Maximum rates depend on plate speeds; minimum rates depend on the ratio of gravity and viscous effects	High and low rates possible
Special features	Cannot reach high strains or steady state; wide range of temperatures is possible; the instrument is commercially available	Often strain is not measured but is calculated from the imposed strain rate; a wide range of temperatures is possible; the instrument is commercially available	Currently limited to room temperature liquids	Is based on a presumed funnel-shaped flow—this may not take place; wide range of temperatures possible

© Faith A. Morrison, Michigan Tech U.

Extensional

Xpansion Instruments
Xpand Your Capabilities

(dual drum windup)

Cambridge Polymer Group, Inc

(filament stretching)

Thermo SCIENTIFIC

(capillary breakup)

TA Instruments

(drum windup)

Measurement of elongational viscosity is still a labor of love.

99

© Faith A. Morrison, Michigan Tech U.

Newer emphasis:

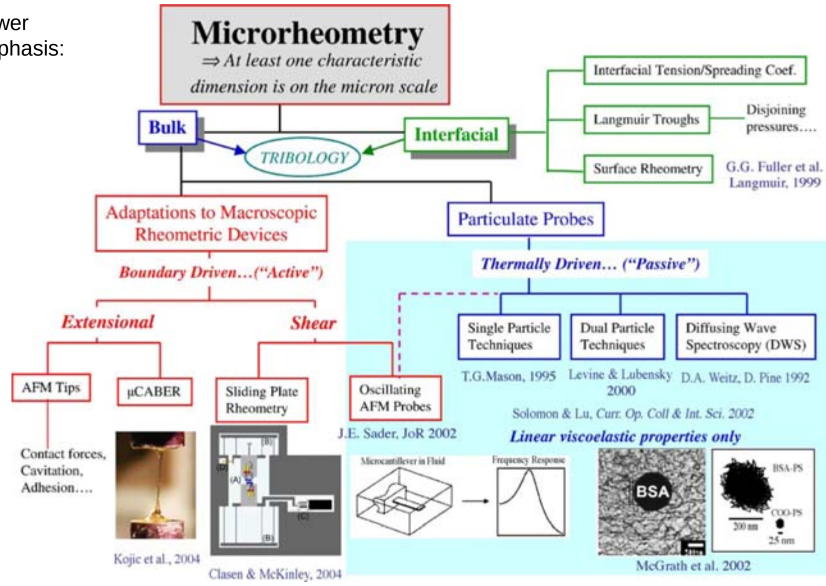

C. Clasen and G. H. McKinley, "Gap-dependent microrheometry of complex liquids," JNNFM, 124(1-3), 1-10 (2004)

100

© Faith A. Morrison, Michigan Tech U.

http://www.ksvnima.com/file/ksv-nima-isrbrochure.pdf

BiolinScientific

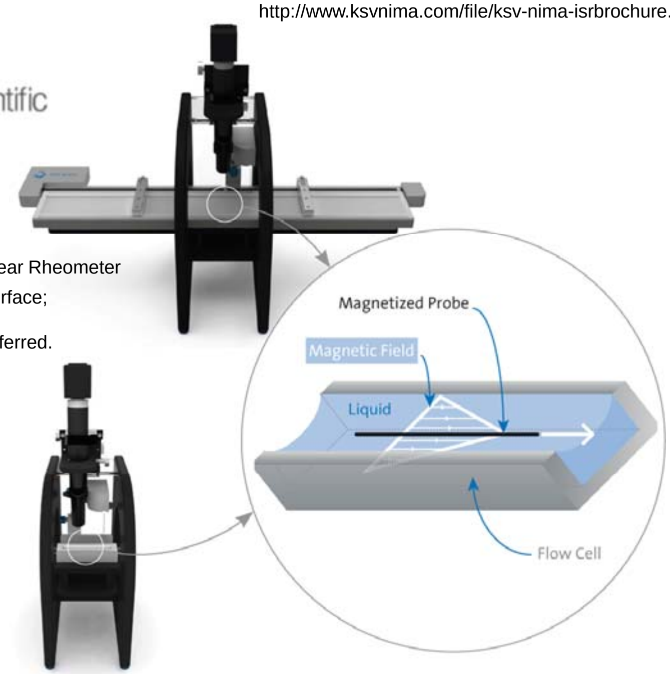

KSV NIMA Interfacial Shear Rheometer

- a probe floats on an interface;
- is driven magnetically;
- material functions are inferred.

© Faith A. Morrison, Michigan Tech U.

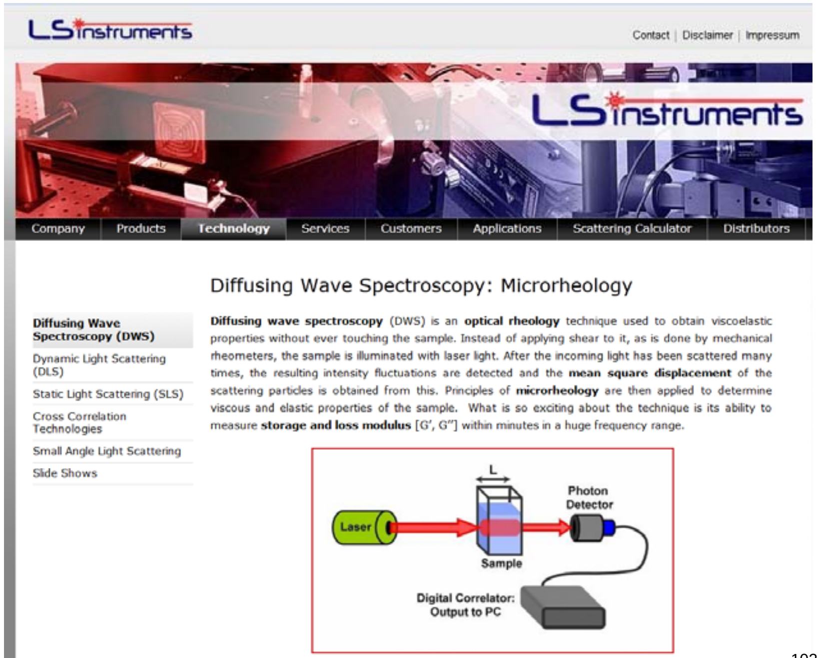

www.lsinstruments.ch/technology/diffusing_wave_spectroscopy_dws/

102

© Faith A. Morrison, Michigan Tech U.

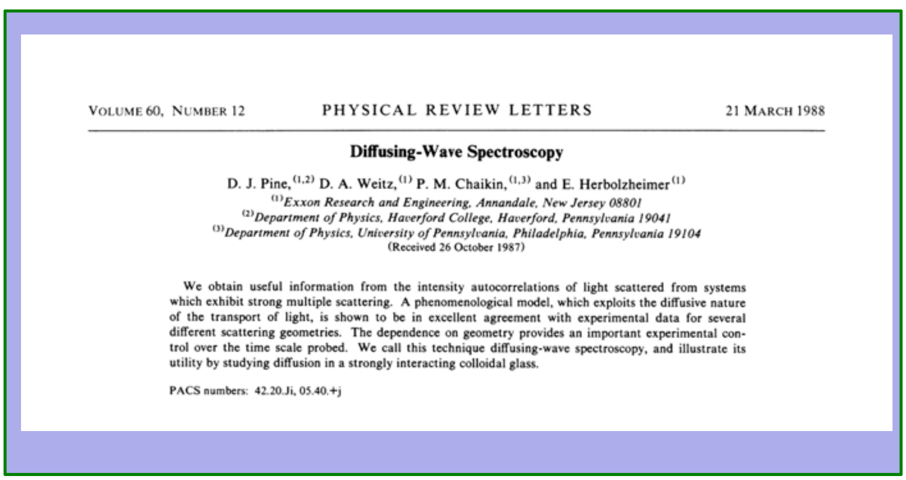

VOLUME 60, NUMBER 12 PHYSICAL REVIEW LETTERS 21 MARCH 1988

Diffusing-Wave Spectroscopy

D. J. Pine,[1,2] D. A. Weitz,[1] P. M. Chaikin,[1,3] and E. Herbolzheimer[1]
[1]*Exxon Research and Engineering, Annandale, New Jersey 08801*
[2]*Department of Physics, Haverford College, Haverford, Pennsylvania 19041*
[3]*Department of Physics, University of Pennsylvania, Philadelphia, Pennsylvania 19104*
(Received 26 October 1987)

We obtain useful information from the intensity autocorrelations of light scattered from systems which exhibit strong multiple scattering. A phenomenological model, which exploits the diffusive nature of the transport of light, is shown to be in excellent agreement with experimental data for several different scattering geometries. The dependence on geometry provides an important experimental control over the time scale probed. We call this technique diffusing-wave spectroscopy, and illustrate its utility by studying diffusion in a strongly interacting colloidal glass.

PACS numbers: 42.20.Ji, 05.40.+j

Strong multiple scattering of light + model = rheological material functions

- D.J. Pine, D.A. Weitz, P.M. Chaikin, and E. Herbolzheimer, "Diffusing-Wave Spectroscopy," *Phys. Rev. Lett.* 60, 1134-1137 (1988).
- Bicout, D., and Maynard, R., "Diffusing wave spectroscopy in inhomogeneous flows," *J. Phys. I* 4, 387–411. 1993

103

© Faith A. Morrison, Michigan Tech U.

Flow Birefringence - a non-invasive way to measure stresses

no net force, isotropic chain,
isotropic polarization

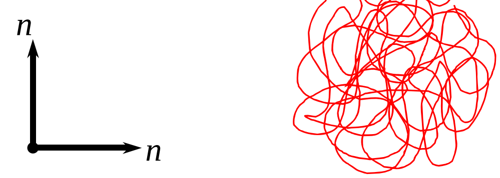

For many polymers, stress and refractive-index tensors are coaxial (same principal axes):

$$\underline{\underline{n}} = C\underline{\underline{\tau}} + B\underline{\underline{I}}$$

Stress-Optical Law

force applied, anisotropic chain,
anisotropic polarization = *birefringent*

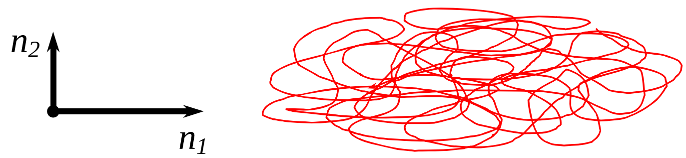

104

© Faith A. Morrison, Michigan Tech U.

Large-Amplitude Oscillatory Shear

A window into nonlinear viscoelasticity

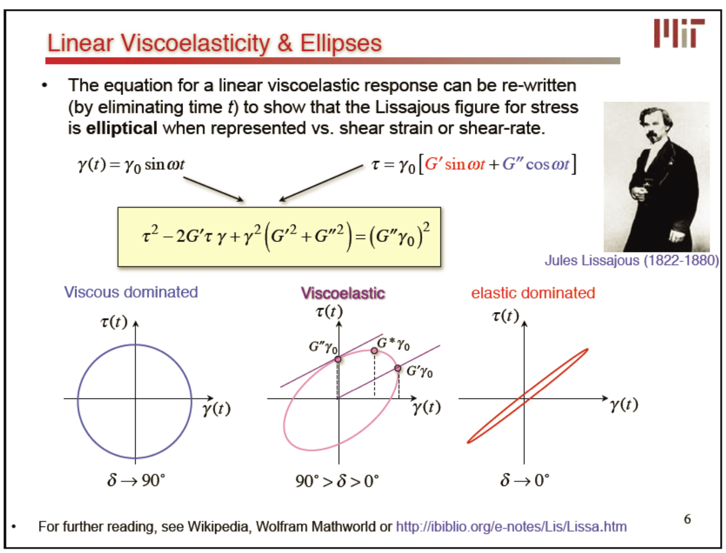

Gareth McKinley, Plenary, International Congress on Rheology, Lisbon, August, 2012
http://web.mit.edu/nnf/ICR2012/ICR_LAOS_McKinley_For%20Distribution.pdf

105

© Faith A. Morrison, Michigan Tech U.

Summary

SHEAR

- Shear measurements are readily made
- Choice of shear geometry is driven by fluid properties, shear rates
- Care must be taken with automated instruments (nonlinear response, instrument inertia, resonance, motor dynamics, modeling assumptions)

- Microrheometry

ELONGATION

- Elongational properties are still not routine
- Newer instruments (Sentmanat,CaBER) have improved the possibility of routine elongational flow measurements
- Some measurements are best left to the researchers dedicated to them due to complexity (FiSER)
- Industries that rely on elongational flow properties (fiber spinning, foods) have developed their own ranking tests

106

© Faith A. Morrison, Michigan Tech U.

Tanner and Walters, *Rheology: An Historical Perspective*, Elsevier, 1998, pp138-9

6.3. Further Commercial Developments on Normal-Stress Measurement

Over the years, the commercial exploitation of the Weissenberg Rheogoniometer has passed through many hands, including, in chronological sequence, Farol Research, Sangamo Controls, Schlumberger, Carrimed and TA. In the early years, the Rheogoniometer was spared any commercial competition. This was to change in the early 70s, with the emergence of "Rheometrics Inc.". The story has its origins at the University of Princeton in the US and involves two young PhD students, Joe Starita and Chris Macosko (see, for example, Macosko and Starita 1971, Starita 1980).

In 1967, Starita completed an MS in Mechanical Engineering working under Bryce Maxwell at Princeton. In the same year, Macosko arrived at Princeton after taking an MSc at Imperial College in the UK. There he was introduced to rheology by Roger Fenner and Gordon Williams; this involved work on a home made cone-and-plate melt rheometer, which used a falling weight to control torque and a mirror to measure rotation.

Both Macosko and Starita were assigned PhD projects which involved the use of the 'Orthogonal Rheometer' that Maxwell had built (see § 6.6). They quickly realised that the existing instrument had serious compliance problems and making this known led to rather heated discussions. However, they decided to redesign the apparatus and persuaded the Department Chairman to purchase a small milling machine, with the argument that, if they failed, it could always be used in the tool shop. They also purchased a wide ranging gear drive and persuaded Triangle Tool Co, where Starita's father worked, to build a stiff X,Y,Z and torque transducer of novel design (US patent 3,693,425).

By early 1969, the new instrument looked promising and Rheometrics was born in early 1970 as a 50/50 partnership between Macosko and Starita. The first instrument was exhibited at the annual US Rheology meeting in Princeton in October 1970. The gears in the original instrument were soon changed to a DC torque motor drive and this provided more flexible speed control.

In 1970, Starita went to work at GE and, six months later, Macosko joined the Faculty of the University of Minnesota. From 1970 to 1972, they both commuted regularly to Triangle Tool Company in New Jersey to supervise the manufacture and testing of the new device.

The so called Mechanical Spectrometer was exhibited at the 1972 International Congress in Lyon, with Imass representing Rheometrics. The response was favourable and everything seemed set for a successful commercial venture. There followed a remarkable series of events.

107

Tanner and Walters, *Rheology: An Historical Perspective*, Elsevier, 1998, pp138-9

Starita decided to start another company to make the Mechanical Spectrometer, leaving Macosko with Rheometrics and a substantial debt. Amongst other things, this series of events led Macosko into a deep Christian faith. One of the fruits of this religious conversion was a willingness to turn over all the stock and the patent rights to Starita.

In 1973, Starita left GE to guide Rheometrics into a successful commercial company and hence provide the makers of the Weissenberg Rheogoniometer with their first effective competition. Macosko was hired as a consultant to the firm and still continues in that role. Starita himself held a prominent leadership position in Rheometrics for over two decades, until he sold his interest in the mid nineties.

Although it may not be immediately apparent from the foregoing discussion, the normal stress facility on what became known as the Rheometrics 'Mechanical Spectrometer' essentially grew out of a rheometer (the Orthogonal Rheometer) which was originally constructed to investigate the linear time dependent behaviour of polymeric systems, through such functions as the storage and loss moduli. In the same way, the third commercial player in the area of all-purpose rheometers, namely Bohlin, entered the field through a restricted rheometrical background. Leif Bohlin had worked in the Department of Food Technology at the Chemical Center, University of Lund, Sweden. There, he had developed a stress-relaxation instrument to investigate the long-time stress-relaxation of wheat flour dough. Later, a controlled-strain oscillation instrument was also developed to study coagulation and gelation of various food-related substances. These developments ultimately led to the construction of the Bohlin VOR rheometer during late 1982 and early 1983, the first commercial instrument being delivered in May 1983. Bohlin resigned his University post in 1984 to devote himself full-time to the fledgling company, Bohlin Rheologi AB.

One stunted development in rheometer development concerns the instrument firm Instron. In 1970, R I Tanner became a rheological consultant to the firm with a view to giving advice on a possible rotary rheometer. Development and design progressed favourably, but there was a hiatus of two years following the launch of the Rheometrics' instrument in 1970; one of the main reasons being the possibility of an Instron buy-out of the fledgling Rheometrics Company. However, no agreement was reached and, after two years, Instron resumed development on the rheometer. By the time the 3250 instrument was ready in 1975, Rheometrics had a five years start. Furthermore, the Instron development was moved to the UK and it is hardly surprising that the instrument failed to make inroads into the expanding US rheometer market - a clear example of the business maxim that 'hesitation is deadly'.

108